International Journal of Engineering

Journal Homepage: www.ije.ir

Analysis of a New Linear Dual Stator Consequent Pole Halbach Array Flux Reversal Machine

N. Arish, H. Yaghobi*

Faculty of Electrical and Computer Engineering, Semnan University, Semnan, Iran

P A P E R I N F O

Paper history:
Received 27 February 2021
Received in revised form 15 June 2021
Accepted 10 July 2021

Keywords:
Finite Element Method
Halbach Array
Linear Machine
Magnetic Orientation
Pm Machine

A B S T R A C T

The permanent magnet machine has attracted much attention due to its high torque density at low speed and simple configuration. This feature is due to many magnetic pole pairs that flux in the air gap can be significantly changed with the smallest motion of the moving. In this paper, a linear dual stator flux reversal permanent magnet machine (LDSFRPMM) with toroidal winding is presented, which magnets embedded with Halbach and simple array on the translator and stator, respectively. The innovation of this structure over a conventional machine is the addition of a magnet between the stator teeth with the appropriate magnetic orientation,and finding the best width of permanent magnet on the stator and a change of the type of winding from the concentrated to the toroidal. By implementing these changes on a conventional machine, the main parameters of the machine such as back electromotive force (EMF), thrust force, power factor and permanent magnetic (PM) flux are increased which improves the performance of the proposed machine.

doi: *10.5829/ije.2021.34.08b.21*

1. INTRODUCTION

In recent years, linear flux reversal permanent magnet machine (LFRPMM) has received considerable research attention. Vernier machine is flag-bearer of this category due to generating high thrust force at the low speed [1, 2]. This feature exists because of numerous magnetic poles which are known as magnetic gearing effect [3, 4]. Generating a high thrust force at the low speed is very efficient in direct drive applications such as wave energy conversion and linear transportation [5, 6]. However, the first linear permanent magnet Vernier machine suffered from poor power factor due to high leakage flux [7]. During the years, scientists have reduced the weakness of the permanent magnetic Vernier machine with a different design. Dual stator spoke array permanent magnet (PM) is one of the most popular designs which is very effective to achieve high power factor, high thrust force and low leakage flux [8]. Recently, engineers by using special material such as superconductor and soft magnetic composite (SMC) improve performance of proposed LDSFRPMM. High-temperature superconductor (HTS) material has been used in electric machines because of high-current tolerance and property of the shield leakage flux [9-12]. Also, SMC material has been used in the structures of PM machine to improve performance of proposed LDSFRPMM in terms of losses and temperature [13, 14]. Copper loss is an important parameter in electrical machine and is significantly related to the type of winding. Based on literature[15, 16], because of the particular type of winding, copper losses in the proposed LDSFRPMM remarkably reduced and thrust force increased. An increase in the volume of the PM and correct selection of the shape of magnet and magnetic direction can improve the performance of the proposed machine [17]. In the various types of structures, magnets are used in the form of simple [18], spoke array [19], skew [20], hybrid [21, 22] and Halbach array [23] to improve the main parameter of the proposed machine. A permanent magnet Vernier machine has been proposed shi et al. [24] and Fan et al. [25]. So that, with an increase in the volume of the PM, air-gap magnetic field, back-EMF and power factor are increased in the proposed machine. Liu et al. [26] by integrating Halbach array leakage flux and the efficiency of the proposed machine have reduced and increased, respectively. Zhao et al. [27]

*Corresponding Author Email: yaghobi@semnan.ac.ir (H.Yaghobi)

Please cite this article as: N. Arish, H. Yaghobi, Analysis of a New Linear Dual Stator Consequent Pole Halbach Array Flux Reversal Machine International Journal of Engineering, Transactions B: Applications, Vol. 34, No. 08, (2021) 2002-2009

by dividing the PM into the very small segment as Halbach array in various magnetic orientation back EMF, thrust force and flux density raised. Nematsaberi and Faiz [28] by changing the simple array to the spoke array PM and applying non-magnetic material the thrust force and PF have increased. The target of this paper is proposing a new LDSFRPMM with toroidal winding and a special arrangement of PM to improve the weaknesses of conventional LDSFRPMM. In the proposed LDSFRPMM magnet with Halbach array is mounted on the translator and simple magnet with correct width and effective orientation is embedded on the stator and winding has changed from concentrated to toroidal. So that, the magnetic orientation of the PM mounted on the stator is the same as the magnetic orientation of the middle part of the magnet with the Halbach array on the translator. In this structure PM flux, air gap flux density, thrust force, power factor and back-EMF are increased which causes the increase of the performance of the proposed LDSFRPMM.

2. MACHINE CONFIGURATION AND OPERATION

Ndfe35 PM with Halbach array is a specific arrangement that compound with several directions like vertical and horizontal. The conclusion of the combination of these two different magnetic directions, is that the intensity of the magnetic field on one side is highly stronger than the other side. All possible magnetic structures such as vertically, horizontally and Halbach are shown in Figure 1. As can be seen, the magnetic field vectors produced by the magnets are symmetric in structures (a) and (b), but in structure (c), they are asymmetric and the magnetic field is stronger on one side than on the other which using this feature properly can improve machine performance By simultaneous use of magnets on stator and translator and proper combination of their magnetic orientation, the proposed LDSFRPMM can reach the ideal sinusoidal magnetic flux, which increases thrust force, PM flux and back-EMF. The proposed LDSFRPMM is designed based upon the conventional LDSFRPMM, which is shown in Figure 2. As can be seen, the main difference between conventional LDSFRPMM and the proposed LDSFRPMM is that there is no magnet on the stator of conventional LDSFRPMM and winding in the proposed LDSFRPMM turns into toroidal from concentrated. So that, in the toroidal winding, each phase consists of one coil, and in the concentrated winding, each phase comprises four coils. Translator is divided into three equal parts, which make the phases separated from each other, and each part consists of four major teeth which each of them are divided into three splits for modulation of the flux**.** The surface of the translator has been covered by a Halbach array composed of the same three magnets with different directions, the central one is vertically magnetized, and the two other sides are horizontally magnetized. PM applied between slots of the stator is magnetized in perpendicular upward and downward directions. The main operation of both machines is based on the effect of the magnetic gear. Because of this effect, with a small displacement of the translator, the flux in the air gap changes rapidly and causes at the low speed to be able to generate high thrust force. The teeth of the stator modulate the PM field to provide an effective magnetic field so that a higher velocity of the field than that of the translator, improves the thrust force. The relation is illustrated by Arish et al. [11] and Yao et al. [29]:

$$p_{pm} = N_s \pm p \quad (1)$$

where P_{pm}, P and N_s are the number of pole pairs on the translator, the number of winding pole pairs and the

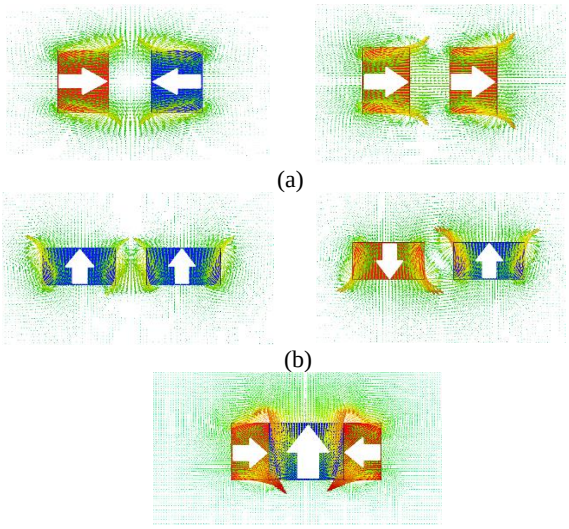

Figure 1. Magnet Structure. (a) Horizontal array, (b) Vertical array, (c) Halbach array

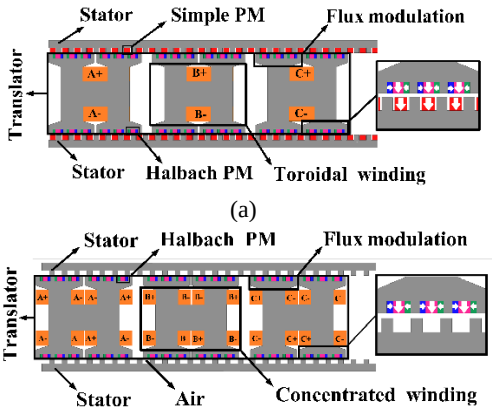

Figure 2. Machine structure. (a) Proposed LDSFRPMM, (b) Conventional LDSFRPMM

number of stator flux modulation teeth respectively in the proposed LDSFRPMM. Magnetic gear ratio is an important design index for the select of slot and pole combinations during the early stages of the machine design. Increasing gear ratio enhances thrust force and back-EMF capability. High thrust force can be achieved with the high number of poles, this typically causes higher leakage flux.

3. PERFORMANCE EVALUATION

In FEM for two machines, the permeability of the iron core is based on practical data, so iron core is laminated and the iron saturation is considered. Adding a magnet on the stator may cause the machine to saturate, which is why it is important to choose the correct magnet width added to the machine. Figure 3 shows the back-EMF and detent force variations based on the millimeter changes of the magnet's width. With magnet's width increases, the trend of detent force is increased too. The magnet width is chosen so that the proposed LDSFRPMM has the low detent force and the highest back-EMF. It should also be noted that the width of the selected magnet does not cause the saturation of the proposed LDSFRPMM. According to the description given, the best selection width is 7 mm. So that for high performance, the magnet width of the Halbach array should satisfy the following relation [3]:

$$w_v + 2w_h < \tau_s \quad (2)$$

$$w_h \leq w_v \quad (3)$$

where w_v , w_h and τ_s are the width of the bigger part of Halbach PM, width of the smaller part of Halbach PM and pole pitch, respectively. To generate a sinusoidal magnetic field in the air-gap, the width of horizontally magnetized PM should be smaller than vertically magnetiz–ed PM. The corresponding mesh of the proposed LDSFRPMM is shown in Figure 4. In order to obtain precise accuracy, more than 10000 meshes in several layers were created and calculated. All the design parameters of the proposed LDSFRPMM and the conventional LDSFRPMM are the same, including current density, translator pole pairs, magnetic gear ratio, the material of the core and air gap length. Design parameter of the proposed LDSFRPMM is shown in Figure 5 and listed in Table 1.

3. 1. Magnetic Field and Air Gap Flux Distribution

The air gap magnetic flux density is directly commensurate to the PM pole pairs in the Vernier machine and generate at the no load state. It is the interaction of the magnetic field generation with the teeth of stator and translator. Figure 6 depicts the waveforms of the air gap magnetic flux, the maximum of magnetic

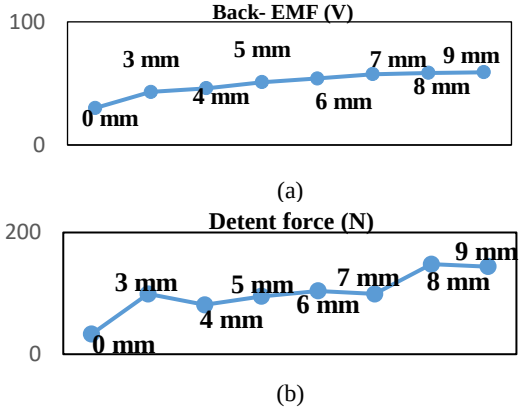

Figure 3. Variation of the back-EMF and detent force respect to width of PM. (a) Back-EMF. (b) Detent force

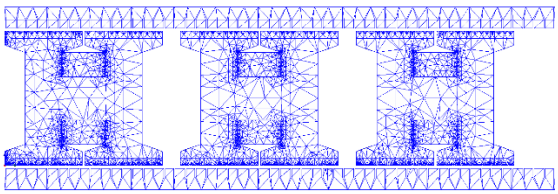

Figure 4. The corresponding mesh of the proposed LDSFRPMM

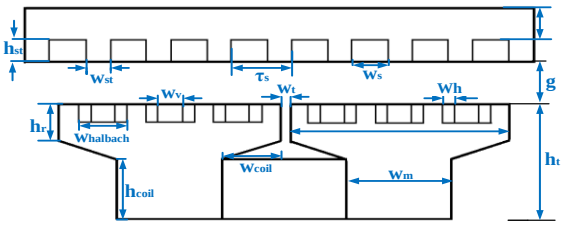

Figure 5. Design parameters of proposed LDSFRPMM

TABLE 1. The design parameter of the proposed LDSFRPMM

Items	Unit	LDSFRPMM
Speed	m/s	1.5
w_h	mm	3
w_v	mm	6
g	mm	2
w_y	mm	10
w_m	mm	26
w_{st}	mm	6
h_{st}	mm	6
h_r	mm	10
h_t	mm	32
w_s	mm	9
w_{coil}	mm	14
h_{coil}	mm	17
$w_{halbach}$	mm	12
τ_s	mm	15

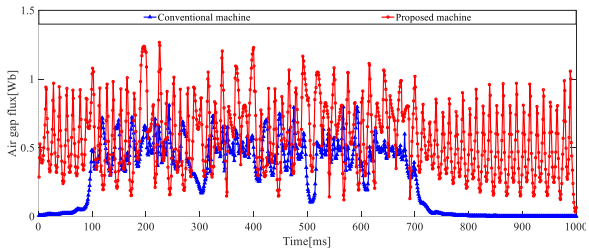

Figure 6. Comparison of the arigap magnetic flux

flux in the air gap for the proposed LDSFRPMM and conventional LDSFRPMM is 1.26 T and 0.81 T, respectively. Hence, the air gap magnetic flux in the proposed LDSFRPMM is 55% higher than the conventional LDSFRPMM. This increase is due to the increased volume of magnets used in the proposed LDSFRPMM. The air gap flux density waveform shows that there is 360 mm effective length, so it contains 24 numbers of the active teeth of the stator. Flux line distribution at the no-load is generated only by PM, and it is shown in Figures 7(a) and 7(b) for two models. It expresses that the flux lines of the three modules in the two models are autonomous. Thus, the field distributions in one phase do not affect relatively on the other phase, therefore the LDSFRPMM possess the excellent fault-tolerant capability. Density of the flux line due to adding the magnet on the stator and changing the type of winding in the proposed LDSFRPMM is higher magnetic flux distribution at full load for the two models generated by PM and armature current simultaneously. Figures 7(c) and 7(d) show magnetic flux distribution at full load for two models. It is evident that the magnetic flux distribution in the proposed LDSFRPMM is higher than conventional LDSFRPMM and maximum magnetic flux density for both models is less than 2. Figure 8 shows the PM flux of two models. PM flux in the proposed LDSFRPMM is generated by PM at the no-load. It is clear that the peak of the PM flux in the proposed LDSFRPMM is higher than the conventional LDSFRPMM, so RMS of the PM flux in the proposed LDSFRPMM and conventional LDSFRPMM are 0.057 Wb and 0.014 Wb, respectively. With an increase in PM flux, the back-EMF also increases accordingly and this improves the power factor and output power of the proposed LDSFRPMM.

3. 2. Back-EMF The relative motion between the translator and stator is caused by the external vibration and magnetic flux through in the air gap will change. Base on the Faraday's law of the electromagnetic induction, the back-EMF will be generated in the coil. The phase's back-EMF can be defined as:

$$EMF = \frac{d\psi}{dt} = \frac{d\psi}{dx}v \quad (4)$$

where, ψ and x are PM flux and displacement, respectively. It is obvious that back-EMF is derivation of PM flux relative to time or derivation of PM flux relative to displacement multiply to velocity. Thus, the back-EMF is only affiliated to the change of PM flux. Figure 9 shows no load back-EMF waveforms for two models. It is obvious which waveform of the back-EMF is purely sinusoidal and acceptable. Because back-EMF is derivation of PM flux, DC part of the PM flux is entirely

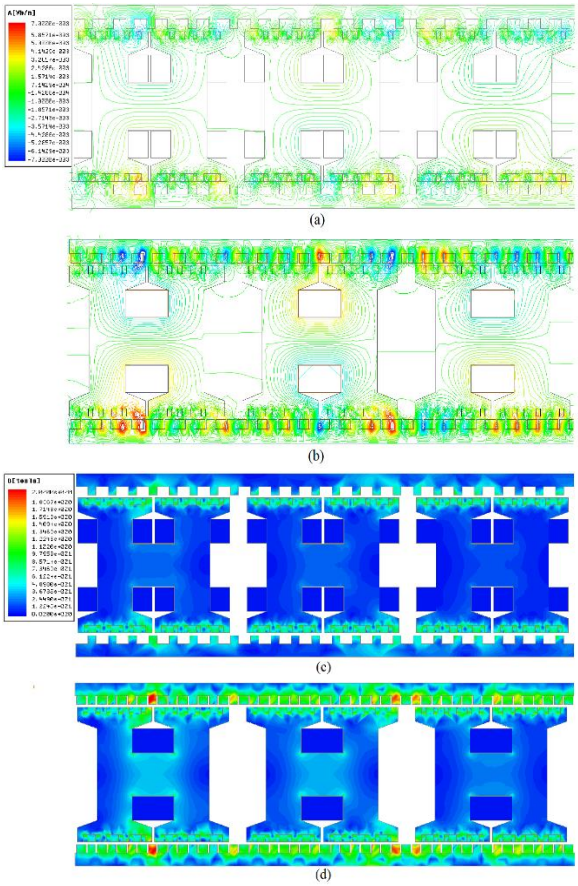

Figure 7. Comparison of the flux density distribution. (a) Flux line distribution in the conventional LDSFRPMM at no load, (b) Flux line distribution in the proposed LDSFRPMM at no load, (c) Magnetic flux distribution in the conventional LDSFRPMM at full load, (d) Magnetic flux distribution in the proposed LDSFRPMM at full load

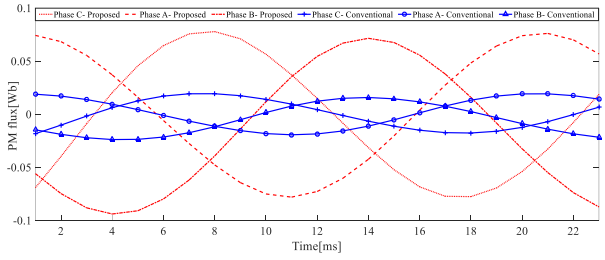

Figure 8. Comparison of the PM flux

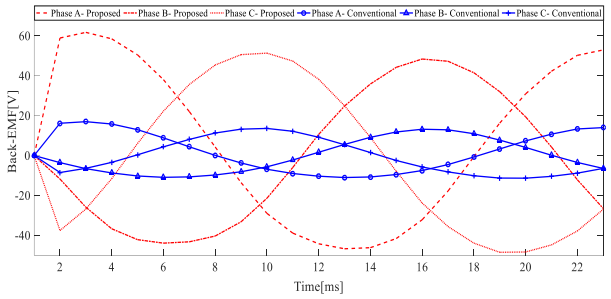

Figure 9. Comparison of the back-EMF

omitted in the waveforms of back-EMF. The maximum of the back-EMF at no load for the proposed LDSFRPMM and conventional LDSFRPMM is 61 V and 17 V, respectively.

In other words, maximum of the back-EMF for the proposed LDSFRPMM is significantly higher than the conventional LDSFRPMM, since the PM volume increases.

3. 3. Self-inductance and Mutual-inductance Self inductance and mutual inductance of the proposed LDSFRPMM and conventional LDSFRPMM are shown in Figure 10. It is obvious that the self-inductance depends on the translator's position and type of winding.

The average of three phases self inductance in the proposed LDSFRPMM and conventional is 35 mH and 8 mH, respectively. As can be seen, the average of three phases self inductance in conventional LDSFRPMM is much less than the proposed LDSFRPMM. Mutual inductance in the proposed LDSFRPMM and conventional LDSFRPMM is approximately equal to zero and mutual inductance between phase a and phase c is lower than two other phases. This is due to the distance between phase a and phase c is longer than two other phases. Because, three phases in both machines are separated and they do not have much impact on each others.

3. 4. Power Factor The classical approach of computing power factor is using phasor diagram which is employed in this paper with irrespective of the stator resistance. Power factor (PF) in LPMVM is given by with assuming that the current i_d is zero [8]:

$$PF = (1+\frac{LsI}{\psi})^{-0.5} \quad (5)$$

where I is the RMS of the phase current and L_s is the synchronous inductance. As can be seen, the major reason for low power factor according to the Equation (5) is high synchronous inductance and low PM flux. The proposed LDSFRPMM can reach high PM flux, because of the increase of volume of the PM and correct magnetic direction of PM. It is true that by converting the winding from the concentrated to the toroidal, the inductance

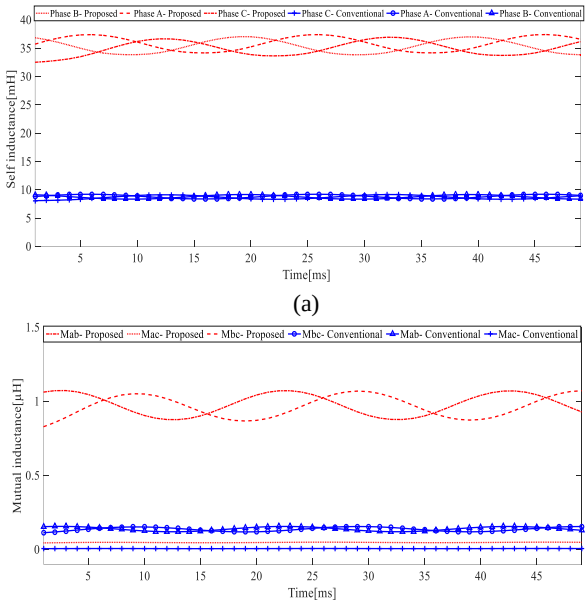

Figure 10. Comparison of inductance. (a) Self inductance. (b) Mutual inductance

increases and this reduces the power factor. But, an increase in the PM flux is much greater than the inductance increase, which according to Equation (5), since the flux is in the denominator of the fraction; generally the power factor is improved.

3. 5. Thrust Force and Detent Force The electromagnetic force for all phases can be defined as follows [3]:

$$F_{ele} = i\frac{d\psi}{dx} + \frac{1}{2}i^2\frac{dL}{dx} + \frac{d}{dx}(\frac{1}{2}i^2L) \quad (6)$$

The first term in Equation (6) is the force generation by PM field and other terms are the forces arising from the position dependent inductances. Hence, the inductance variations with translator position in the proposed LDSFRPMM may give increase to fluctuating force. For both models, the thrust force can be given by Botha et al. [31]:

$$F_{thrust} = F_{ele} + F_{detent} \quad (7)$$

Detent force is a drawback for the linear machine which leads to mechanical vibration and noise for the machine. Then, minimizing detent force is an important requirement for linear machine design. Detent force in linear permanent magnet machine is appeared by two main reasons: 1- slot effect 2- end effect. Slot effect in the linear machine is caused by the interaction of PMs and the iron teeth. Also, the end effect is caused by the finite stator core length and has an impact on phase a and

phase c. Therefore, the electromagnetic parameters of phase b are higher than other phases. Figures 11(a) and 11(b) depict the detent force and thrust force for both models at the no-load and full load, respectively. As can be seen, the value of the detent force in the proposed LDSFRPMM is higher than conventional LDSFRPMM, but the average of thrust force in the proposed LDSFRPMM is higher than conventional LDSFRPMM and average of the thrust force for the proposed LDSFRPMM and conventional LDSFRPMM is 415 N and 50 N, respectively. High thrust force density of the proposed LDSFRPMM is due to the increase of volume of the PM and type of winding which causes flux density in yoke of the proposed LDSFRPMM be higher than yoke of conventional LDSFRPMM. High ripple force reduces machine performance, when the d-axis current is zero, the ripple of thrust force is obtained [32]:

$$F_{thrust} = \frac{F_{max} - F_{min}}{F_{avg}} \times 100\% \quad (8)$$

where, F_{max} is maximum thrust force, F_{min} is minimum thrust force, and F_{avg} is average thrust force. The ripple of thrust force in the proposed LDSFRPMM is a little higher than conventional LDSFRPMM which it is non-important at the low speed. It should be noted that with the increase of the PM volume, PM flux, back-EMF, thrust force, power factor and air gap flux density increase too. For a better comparison, the electromagnetic parameters of the proposed LDSFRPMM and conventional LDSFRPMM are presented in Table 2.

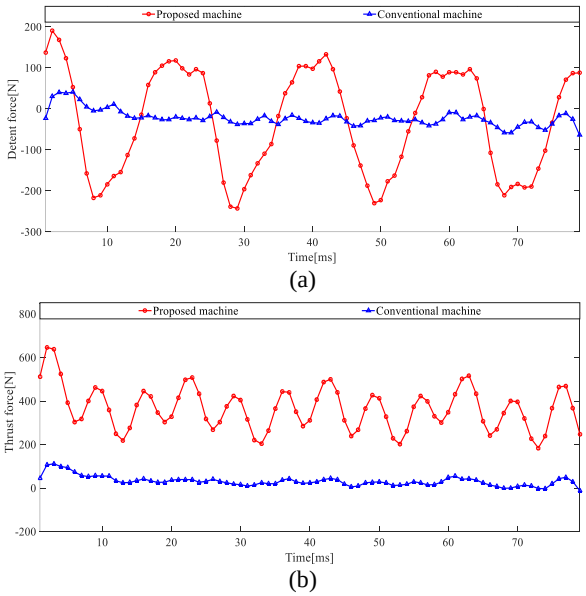

Figure 11. Comparison of force. (a) Detent force, (b) Thrust force

TABLE 2. Electromagnetic performance comparison

Item	Proposed LDSFRPMM	Conventional LDSFRPMM
Air gap flux density (T)	1.26	0.81
PM flux linkage (Wb)	0.057	0.014
Back-EMF (V)	61	17
Self-inductance (mH)	35	8
Thrust force (N)	415	50

4. CONCLUSION

This paper proposes a new LDSFRPMM topology with toroidal winding which simple PM with correct orientation and width is mounted on the stator and Halbach array PM is mounted on the translator. This paper shows the importance of width of magnet and winding arrangement. Electromagnetic performance of the proposed LDSFRPMM was compared to conventional LDSFRPMM by FEM in terms of back-EMF, thrust force, detent force, inductance, power factor, air gap flux density and PM flux. According to the obtained results of FEM, the novelty improved the performance of the proposed LDSFRPMM compared to conventional LDSFRPMM. So that, airgap flux density in the proposed LDSFRPMM and conventional LDSFRPMM is 1.26 T and 0.81 T, respectively. PM flux in the proposed LDSFRPMM and conventional LDSFRPMM is 0.057 Wb and 0.014 Wb, respectively. Back-EMF in the proposed LDSFRPMM and conventional LDSFRPMM is 61 V and 17 V, respectively. Inductance in the proposed LDSFRPMM and conventional LDSFRPMM is 35 mH and 8 mH, respectively. Thrust force, in the proposed LDSFRPMM and conventional LDSFRPMM, is 415 N and 50 N, respectively. In addition, the thrust force of the proposed LDSFRPMM has a significant increase compared to the conventional LDSFRPMM.

5. REFERENCES

1. Toba, A., and T. A. Lipo. "Novel Dual-Excitation Permanent Magnet Vernier Machine" Conference Record of the 1999 IEEE Industry Applications Conference. Thirty-Forth IAS Annual Meeting, Vol. 4, (1999), 2539-2544, doi:10.1109/IAS.1999.799197.
2. Raza, M., Zhao, W., Lipo, T.A. and Kwon, B.I., "Performance Comparison of Dual Airgap and Single Airgap Spoke-Type Permanent-Magnet Vernier Machines." ***IEEE Transactions on Magnetics***, Vol. 53, No. 6, (2017), doi:10.1109/TMAG.2017.2669105.
3. Ji, J., Zhao, W., Fang, Z., Zhao, J. and Zhu, J., "A Novel Linear Permanent-Magnet Vernier Machine With Improved Force Performance" ***IEEE Transactions on Magnetics***, Vol. 51, No. 8, (2015), doi:10.1109/TMAG.2015.2416123.
4. Ho, S.L., Niu, S. and Fu, W.N. "Design and Comparison of

Vernier Permanent Magnet Machines" ***IEEE Transactions on Magnetics***, Vol. 47, No. 10, (2011), 3280-83, doi:10.1109/TMAG.2011.2157309.

5. Faiz, J. and A. R. Nematsaberi. "Linear Electrical Generator Topologies for Direct-Drive Marine Wave Energy Conversion-an Overview" ***IET Renewable Power Generation***, Vol. 11, No. 9, (2017), 1163-76, doi:10.1049/iet-rpg.2016.0726.
6. Du, Y., Cheng, M., Chau, K.T., Liu, X., Xiao, F. and Zhao, W., "Linear Primary Permanent Magnet Vernier Machine for Wave Energy Conversion" ***IET Electric Power Applications***, Vol. 9, No. 3, (2015), 203-212, doi:10.1049/iet-epa.2014.0138.
7. Li, X., tong Chau, K., Cheng, M., Kim, B. and Lorenz, R.D. "Performance Analysis of a Flux-Concentrating Field-Modulated Permanent-Magnet Machine for Direct-Drive Applications" ***IEEE Transactions on Magnetics***, Vol. 51, No. 5, (2015), doi:10.1109/TMAG.2014.2374553.
8. Li, D., Qu, R. and Lipo, T.A., "High-power-factor vernier permanent-magnet machines" ***IEEE Transactions on Industry Applications,*** Vol. 50, No. 6, (2014), 3664-3674. DOI:10.1109/TIA.2014.2315443.
9. Ardestani, M., Arish, N. and Yaghobi, H., "A new HTS dual stator linear permanent magnet Vernier machine with Halbach array for wave energy conversion" ***Physica C: Superconductivity and its Applications,*** Vol. 567, No. 12, (2020). DOI:10.1016/j.physc.2019.1353593.
10. Arish, N., "Electromagnetic performace analysis of linear vernier machine with PM and HTS-Bulk" ***Physica C: Superconductivity and its Applications,,*** Vol. 579, (2020). doi.org/10.1016/j.physc.2020.1353751
11. Arish, N., Ardestani, M., and Hekmati, A., " Study on the optimum structure of the rotor slot shape for a 20-kW HTS", ***Physica C: Superconductivity and its Applications,*** Vol. 567, (2021), doi.org/10.1016/j.physc.2021.1353829.
12. Arish, N., Marignetti, F and Yazdani-Asrami, M. " Comparative study of a new structure of HTS-bulk axial flux-switching machine" ***Physica C: Superconductivity and its Applications,*** Vol. 584, (2021). doi.org/10.1016/j.physc.2021.1353854
13. Marignetti, F., Colli, V.D. and Coia, Y., "Design of Axial Flux PM Synchronous Machines through 3-D Coupled Electromagnetic Thermal and Fluid-Dynamical Finite-Element Analysis" l***EEE Transactions on Industrial Electronics***, Vol. 55, No. 10, (2008), 3591-3601, doi:10.1109/TIE.2008.2005017.
14. Kim, C.W., Jang, G.H., Kim, J.M., Ahn, J.H., Baek, C.H. and Choi, J.Y., "Comparison of Axial Flux Permanent Magnet Synchronous Machines with Electrical Steel Core and Soft Magnetic Composite Core" ***IEEE Transactions on Magnetics***, Vol. 53, No. 11, (2017), 1-4., doi:10.1109/TMAG.2017.2701792.
15. Bian, F. and Zhao, W., "A new dual stator linear permanent-magnet vernier machine with reduced copper loss", ***AIP Adv,*** Vol. 7, No. 5, (2017). DOI:10.1063/1.4978589.
16. Arish, N., Ardestani, M. and Teymoori, V., "Comparison of Dual Stator Consequent-Pole Linear Permanent Magnet Vernier Machine with Toroidal and Concentrated Winding" 2020 11th Power Electronics, Drive Systems, and Technologies Conference, PEDSTC 2020, (2020), doi:10.1109/PEDSTC49159.2020.9088384.
17. Arish, N. and Marignetti, F. "Evaluation of Linear Permanent Magnet Vernier Machine Topologies for Wave Energy Converters" ***International Journal of Engineering, Transactions B: Applications***, Vol. 34, No. 2, (2021) 403-413, doi:10.5829/IJE.2021.34.02B.12
18. Almoraya, A.A., Baker, N.J., Smith, K.J., and Raihan, M.A.H., "Design and Analysis of a Flux-Concentrated Linear Vernier Hybrid Machine with Consequent Poles", ***IEEE Transactions on Industry Applications,*** Vol. 55, No. 5, (2019), 4595-4604. DOI:org/10.1109/TIA.2019.2918499.
19. Zhu, X., Ji, J., Xu, L. and Kang, M., "Design and Analysis of Dual-Stator PM Vernier Linear Machine with PMs Surface-Mounted on the Mover" ***IEEE Transactions on Applied Superconductivity***, Vol. 28, No. 3 2018, doi:10.1109/TASC.2017.2786713.
20. S. Khaliq, F. Zhao and B. Kwon, "Design and analysis of a dual stator spoke type linear vernier machine for wave energy extraction," 2015 IEEE International Magnetics Conference, (2015), doi: 10.1109/INTMAG.2015.7157480
21. Arish, N., Teymoori, V., Yaghobi, H. and Moradi, "Design of New Linear Vernier Machine with Skew and Halbach Permanent Magnet for Wave Energy Converters." 34th International Power System Conference, PSC 2019, (2019), doi:10.1109/PSC49016.2019.9081549.
22. Arish, N and Teymoori, V., "Development of Linear Vernier Hybrid Permanent Magnet Machine for Wave Energy Converter" ***International Journal of Engineering, Transaction B: Applications***, Vol. 33, No. 5, (2020), 805-813. doi.org/10.5829/ije.2020.33.05b.12.
23. Ho, S.L., Wang, Q., Niu, S. and Fu, W.N., "A Novel Magnetic-Geared Tubular Linear Machine with Halbach Permanent-Magnet Arrays for Tidal Energy Conversion" ***IEEE Transactions on Magnetics***, Vol. 51, No. 11, (2015), doi:10.1109/TMAG.2015.2450720.
24. Shi, C., Li, D., Qu, R., Zhang, H., Gao, Y. and Huo, Y., "A Novel Linear Permanent Magnet Vernier Machine with Consequent-Pole Permanent Magnets and Halbach Permanent Magnet Arrays." ***IEEE Transactions on Magnetics***, Vol. 53, No. 11, (2017), doi:10.1109/TMAG.2017.2696559.
25. Fan, H., Chau, K.T., Cao, L. and Jiang, C., Machine." ***IEEE Transactions on Energy Conversion***, Vol. 33, No. 4, (2018), 2081-2090, doi:10.1109/TEC.2018.2848545.
26. G. Liu, H. Zhong, L. Xu and W. Zhao, "Analysis and Evaluation of a Linear Primary Permanent Magnet Vernier Machine With Multiharmonics," ***in IEEE Transactions on Industrial Electronics,*** Vol. 68, No. 3, (2021), 1982-1993, doi: 10.1109/TIE.2020.2973888.
27. Zhao, W., Zheng, J., Wang, J., Liu, G., Zhao, J. and Fang, Z., "Design and analysis of a linear permanent- magnet vernier machine with improved force density", ***IEEE Transactions Industrial Electronics***, Vol. 63, No. 4, (2016), 2072-2082. doi.10.1109/TIE.2015.2499165.
28. Nematsaberi, A. and Faiz, J., "A Novel Linear Stator-PM Vernier Machine With Spoke- Type Magnets", l***EEE Transactions on Magnetics***, Vol. 54, No. 11, (2018), 1-5. doi.org/10.1109/iraniancee.2019.878640.
29. Yao, T., Zhao, W., Bian, F., Chen, L. and Zhu, X., "Design and Analysis of a Novel Modular-Stator Tubular Permanent-Magnet Vernier Motor." ***IEEE Transactions on Applied Superconductivity,*** Vol. 28, No. 3, (2018), doi:10.1109/TASC.2018.2797948.
30. Li, D., Qu, R. and Zhu, Z., "Comparison of Halbach and Dual-Side Vernier Permanent Magnet Machines" ***IEEE Transactions on Magnetics***, Vol. 50, No. 2, (2014), doi:10.1109/TMAG.2013.2280760.
31. Botha, C.D., Kamper, M.J., Wang, R.J. and Sorgdrager, A.J., "Force Ripple and Cogging Force Minimisation Criteria of Single-Sided Consequent-Pole Linear Vernier Hybrid Machines." Proceedings - 2020 International Conference on Electrical Machines, ICEM 2020, (2020), doi:10.1109/ICEM49940.2020.9270845.
32. Davari, H., and Y. Alinejad-Beromi. "Torque Ripple Reduction in Switched Reluctance Motors by Rotor Poles Shape and Excitation Pulse Width Modification." ***Iranian Journal of Electrical and Electronic Engineering***, Vol. 16, No. 1, (2020), 122-129, doi:10.22068/IJEEE.16.1.122.

Persian Abstract

چکیده

ماشین آهنربای دائمی به دلیل تراکم گشتاور بالا در سرعت کم و پیکربندی ساده توجه بسیاری را به خود جلب کرده است .این ویژگی به دلیل تعداد زیادی جفت قطب مغناطیسی است که شار در شکاف هوا می تواند با کوچکترین حرکت متحرک به صورت قابل توجهی تغییر کند .در این مقاله ، یک ماشین آهنربای دائمی شار برگشت استاتور دوبل خطی با سیم پیچ توروئیدال ارائه شده است که آهن ربا ها به ترتیب با آرایش هالباخ و ساده روی متحرک و استاتور نصب شده است .نوآوری این ساختار بر روی یک ماشین معمولی افزودن آهنربا بین دندانهای استاتور با جهت گیری مغناطیسی مناسب و تغییر نوع سیم پیچ از متمرکز به توروئیدال است .با اجرای این تغییرات بر روی یک ماشین معمولی ، پارامترهای اصلی دستگاه مانند نیروی الکتروموتور، نیروی رانش ، ضریب توان و شار مغناطیسی دائمی افزایش می یابد که باعث بهبود عملکرد ماشین پیشنهادی می شود.